Angewandte Chemie
Eine Zeitschrift der Gesellschaft Deutscher Chemiker

Supporting Information

Making or Breaking Metal-Dependent Catalytic Activity: The Role of Stammers in Designed Three-Stranded Coiled Coils

*Tyler B. J. Pinter, Elizabeth C. Manickas, Audrey E. Tolbert, Karl J. Koebke, Aniruddha Deb, James E. Penner-Hahn, and Vincent L. Pecoraro**

ange_202008356_sm_miscellaneous_information.pdf

Supporting Information
Table of Contents

Experimental Procedures

General Methods: All reagents were purchased from Sigma-Aldrich or Fisher Scientific and used as supplied unless otherwise indicated. All samples containing Cu(I) were prepared in a $N_{2(g)}$ glove box.

Synthesis and purification of peptide: Peptides were synthesized using standard Fmoc chemistry solid phase peptide synthesis on a Rink Amide Methylbenzhydrylamine (MBHA) resin with a Biotage Initiator+Alstra microwave synthesizer following previously reported procedures.[1] The crude peptide was simultaneously cleaved and deprotected using a cleavage cocktail consisting of trifluoroacetic acid (TFA), ethanedithiol, anisole, and thioanisole (90:3:2:5). The peptide was precipitated with cold diethyl ether, recovered by vacuum filtration, dissolved in 50% acetonitrile in ddH_2O and lyophilized to dryness. The lyophilized crude product was then redissolved in 10% acetic acid in ddH_2O and loaded onto a 300 mm x 50 mm DeltaPAK preparative C18 column using a Waters 600 HPLC system with the following parameters: flow rate: 20 mL/min, solvent A: 0.1% TFA in water, solvent B: 0.1% TFA in (90:10) CH_3CN:H_2O, linear gradient: 70:30 (A:B) increasing to 20:80 over 35 min. and fractions containing pure peptide were combined and lyophilized to yield pure, white powder. The dried peptide was stored at -80°C until use. Purity and identity were confirmed using an Agilent Q-TOF ESI-MS operated in positive ion mode.

Spectroscopy: UV visible absorption data were collected with a Cary 100 spectrometer at room temperature in 10 mm quartz cuvettes. CD data were collected on a Jasco J-1500 CD spectropolarimeter with an ATS-530 automatic titrator for guanidinium titrations. Electron paramagnetic resonance spectral data were collected using a Bruker EMXE 200 EPR spectrometer on solutions containing 1 mM peptide, 750 µM Cu(II)Acetate, 30% glycerol, and 50 mM MES at pH 5.8. The EPR spectra were processed using the software SpinCount[2]. The simulations were also performed using SpinCount to determine the g∥, g⊥, A∥, and A⊥ values.

K_d determinations: Cu(I) binding constants were determined by competitive titration with bathocuproinedisulfonate disodium salt (Na_2BCS, $\log\beta_2 = 19.8$[3]) in 50 mM MES buffer pH 5.9 monitored with UV spectroscopy. Cu(II) binding constants were determined by tryptophan fluorescence quenching in 50 mM MES pH 5.9 buffer as previously described.[4] Zn(II) binding constants were determined by competitive titration with zincon ($K_{d,app} = 5.90 \times 10^{-9}$ M[5]) in 50 mM CHES pH 9.5 buffer as previously described[6].

CuNiR activity: Background corrected NiR activity was measured by UV-Visible spectroscopy using previously published procedures[7] monitoring ascorbate oxidation. Pseudo first order rate constants were determined in solutions containing ~30 mM nitrite, ~1.2 mM ascorbate and varying metallopeptide catalyst.

pNPA esterase activity: The background corrected esterase activities were determined following published procedures[8] with p-nitrophenyl acetate as the substrate in 50 mM CHES, pH 9.5 at room temperature.

X-ray absorption spectroscopy: Samples with final concentrations of 1 mM metal, 1.5 mM 3SCC (4.5 mM peptide), 50 mM buffer, and 50% glycerol (as a glassing agent) were prepared, pH adjusted, loaded into an XAS sample cell, and frozen in liquid nitrogen for transport and analysis. Sub-stoichiometric concentrations of metal were used to ensure limited amounts of non-peptide associated metal. To limit photoreduction of Cu(II) samples, multiple scans were performed on different locations of the sample cuvette, scans were overlaid and any showing photoreduction were not used for analysis.

All XAS measurements were performed at Stanford Synchrotron Radiation Lightsource (SSRL) Beam line 9-3. A Si(220) double crystal monochromator was utilized, with a flat Rh-coated vertically collimating harmonic rejection monochromator. The X-ray energy was calibrated by collecting the absorption spectrum of a reference metal foil, placed between two ionization chambers situated behind the sample, at the same time as the fluorescence data were collected, with the first inflection point of the foil assigned as 8980.3 eV for Cu and 9663.7 eV for Zn. The samples were maintained at a temperature of ~7-10 K during data acquisition using a liquid helium cryostat, and the data were measured in fluorescence mode with a 100-element energy resolving Ge detector. The data were collected using 0.25 eV steps in the XANES region (1 sec. integration time), and 0.05 $Å^{-1}$ increments for the extended X-ray absorption fine structure

(EXAFS) region up to k=13.5 $Å^{-1}$, with an integration times of 1-20 s (k^3 weighted) in the EXAFS region. The maximum incident count rate for the channel with the highest counts was kept below 10,000 to avoid detector saturation. The EXAFS data were analyzed using the EXAFSPAK[9] suite of programs with FEFF version 9.0[10]. XANES data were normalized with MBACK.[11] The data were processed with threshold energy, E_0, 9000 eV for Cu and 9680 eV for Zn to convert raw data to k-space, and the background was removed using a 3-region cubic spline. The models were fit with ΔE_0 fixed to -10 eV.

Creation of structural model for ***GR****W$_{27stamAEL}$L33H:* The X-ray structures of the crystallographic analogue of **GR**W-H, Pb_S,Zn_N-**GRCS** L16CL30H (5KB0[12]) and of the stammer region of the 3SCC domain of ORF1p (6FIA[13]) were used. The 5KB0 structure was imported into Pymol (v 2.5[14]) the symexp command was used to reproduce the crystallographic symmetric 3SCC structure. Then the Pb was removed and Cys16 was mutated back to Leu using the Pymol mutate plugin. The stammer (residues 91-93, MEL extracted from 6FIA) were also loaded and a M91A mutation was performed using the Pymol mutate plugin. These three residues (AEL) were inserted into the correct position of the 3SCC sequence using the align command of Pymol to generate a starting model with the correct sequence of a crystallographic analogue of **GR**W$_{27stamAEL}$L33H. Thus, our model is a chimera of previously published X-ray structures. The model was geometry minimized in UCSF Chimera (v1.14[15]) using GAFF[16] and Antechamber[17] with 10,000 steps of steepest decent followed by 1,000 steps of conjugate gradient minimization.

SUPPORTING INFORMATION

Supplementary Tables (S1-S2)

Table S1. EXAFS model fit parameters for Cu(I) at pH 5.8, Cu(II) at pH 5.8 and Zn(II) at pH 9.5 bound to **GR**$W_{27stamAEL}$L33H. The fits highlighted are those discussed in the main text and these fits are shown in Figure S3.

Construct	Model	M-O R[a] (Å)	M-O σ^{2} [b] × 10^{-3} (Å^2)	Cu-N R[a] (Å)	Cu-N σ^{2} [b] × 10^{-3} (Å^2)	Goodness of Fit
Cu(I)	CuHis	-	-	1.886	5.69	144.9
	$CuHis_2$	-	-	1.890	7.34	139.9
	$CuHis_2O$	1.886	1.60	1.927	45.13	86.1
	$CuHis_2O_2$	1.890	5.40	2.159	14.13	103.1
	$CuHis_3$	-	-	1.890	10.70	145.3
	$CuHis_3O$	1.887	1.62	1.928	45.29	87.0
	$CuHis_3O_2$	1.460	98.50	1.888	11.76	134.9
Cu(II)	CuHis	-	-	1.930	2.0	269.2
	$CuHis_2$	-	-	1.931	4.94	197.7
	$CuHis_2O$	1.908	1.45	1.953	7.38	139.0
	$CuHis_2O_2$	1.932	2.96	1.963	22.00	184.9
	$CuHis_3$	-	-	1.932	7.07	183.5
	$CuHis_3O$	1.927	-.60	1.959	16.85	143.5
	$CuHis_3O_2$	1.930	2.38	2.065	58.07	192.5
Zn(II)	ZnHis	-	-	1.998	2.63	470.9
	$ZnHis_2$	-	-	1.994	5.65	347.3
	$ZnHis_2O$	2.002	2.24	1.982	9.08	203.5
	$ZnHis_2O_2$	2.015	3.88	1.948	11.65	164.2
	$ZnHis_3$	-	-	1.988	7.40	281.7
	$ZnHis_3O$	1.991	3.21	1.982	10.62	188.9

[a] R = scatterer distance. [b] σ^2 = Debye Waller Factor

The highlighted fits (shown also in Table 3) are chemically plausible. However, as shown above, they are only marginally better than alternative possibilities. It is noteworthy that the average nearest-neighbor distance is not sensitive to the model that is used. No fit using fewer than 2 histidines was able to account for the observed outer shell scattering (Fig. S3).

SUPPORTING INFORMATION

Table S2. Spectroscopic parameters at pH 5.8 for Cu(II) bound peptides

Construct	λ_{max} (nm)	ε_{λ} ($M^{-1}cm^{-1}$)	g_x, g_y, g_z	A_{II}
TRIW-H[a]	643	135	2.064, 2.028, 2.271	167
GR$W_{27stamAEL}$L33H	645	140	2.045, 2.045, 2.280	173

[a] From Ref.[18]

SUPPORTING INFORMATION

Supplementary Figures (S1-S10)

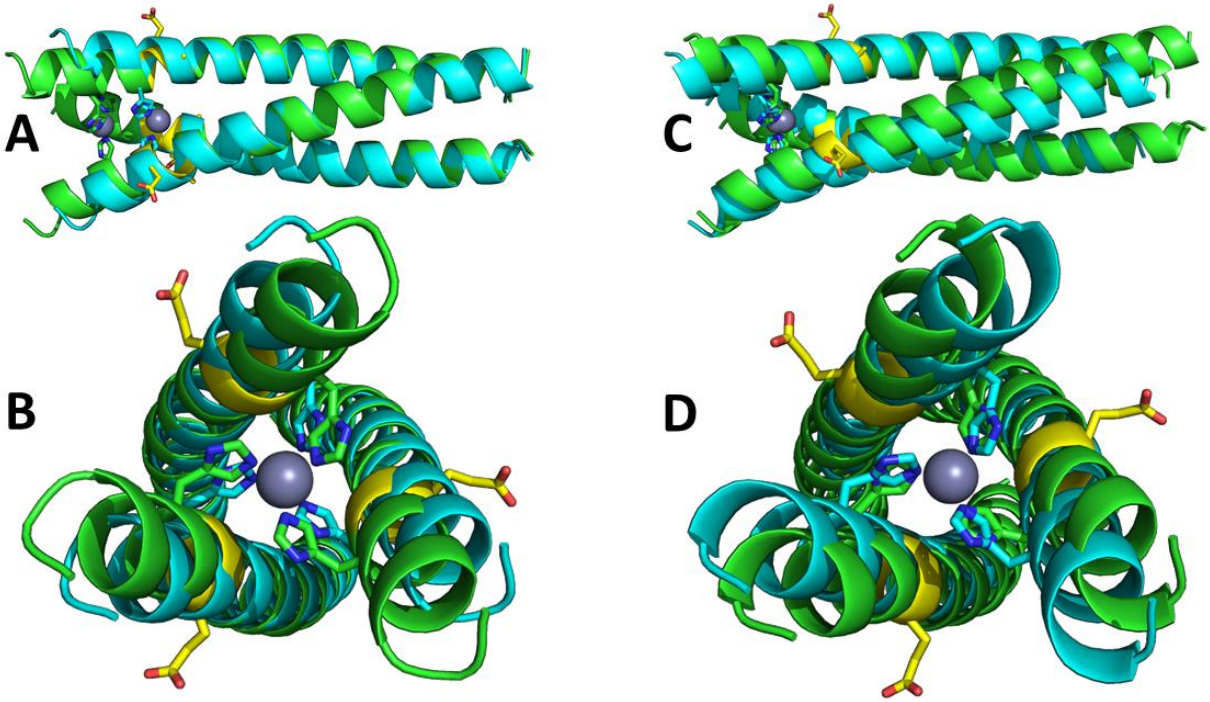

Figure S1. Overlays of **GR**W$_{27stamAELi}$33H model structure (green) with the crystallographic parent of the model 5KB0[12] (cyan). Panels A and B show the alignment of the N-terminal pre-stammer region of the model with the parent. These panels show the position of the stammer within the 3SCC and how stammer insertion causes a change in the overall 3SCC helical topology due to the 3_{10}-helical region of the stammer. Panels C and D show an alternative alignment using the zinc and zinc-coordinating εN of the zinc-coordinating His residues. These panels show that there is a different positioning of the His within the 3SCC upon stammer insertion due to local distortions. This is evidenced by the different positions of the Cα and Cβ carbon of the His residues. Panel A and C show the 3SCCs form the side, with the C-termini to the left. Panels B and D are shown looking from the N-termini up the 3-fold helical axis. The stammer region of **GR**W$_{27stamAEL}$I33H is shown in yellow (the 310 region is narrowed in diameter and stretched compared to the rest of the α-helix), with the side chains shown as sticks. The zinc coordinating His residues (H33 for **GR**W$_{27stamAEL}$I33H and H30 for the parent) are shown as sticks with the zinc shown as grey spheres Details on the model creation are provided in the methods section.

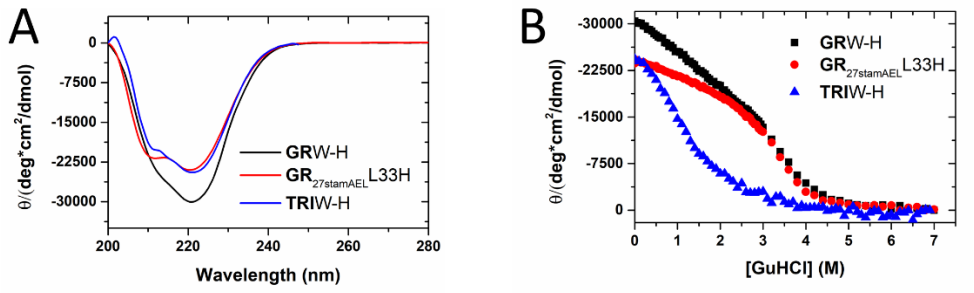

Figure S2. CD spectral data (A) and guanidinium unfolding (B) results for **GR**W-H, **GR**W$_{27stamAEL}$L33H, and **TRI**W-H. Conditions: 15 μM peptide (5 μM 3SCC) in 10 mM potassium phosphate, pH 7.5. Spectra were recorded at room temperature

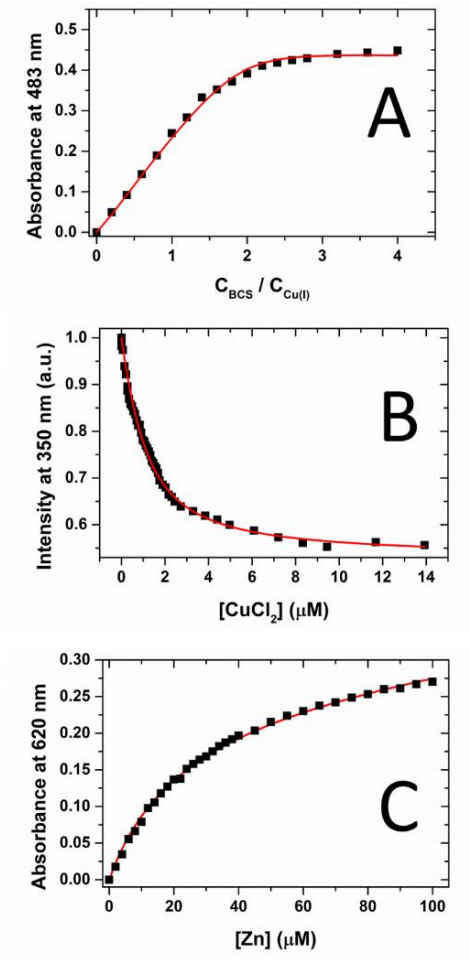

Figure S3: Example datasets and curve fits for determining the metal affinities to **GR**$W_{27stamAEL}$L33H for Cu(I) using competitive BCS titration (A), Cu(II) using tryptophan quenching (B), and Zn(II) using competition with zincon (C). The data are shown as black squares and the fits are shown as solid red lines.

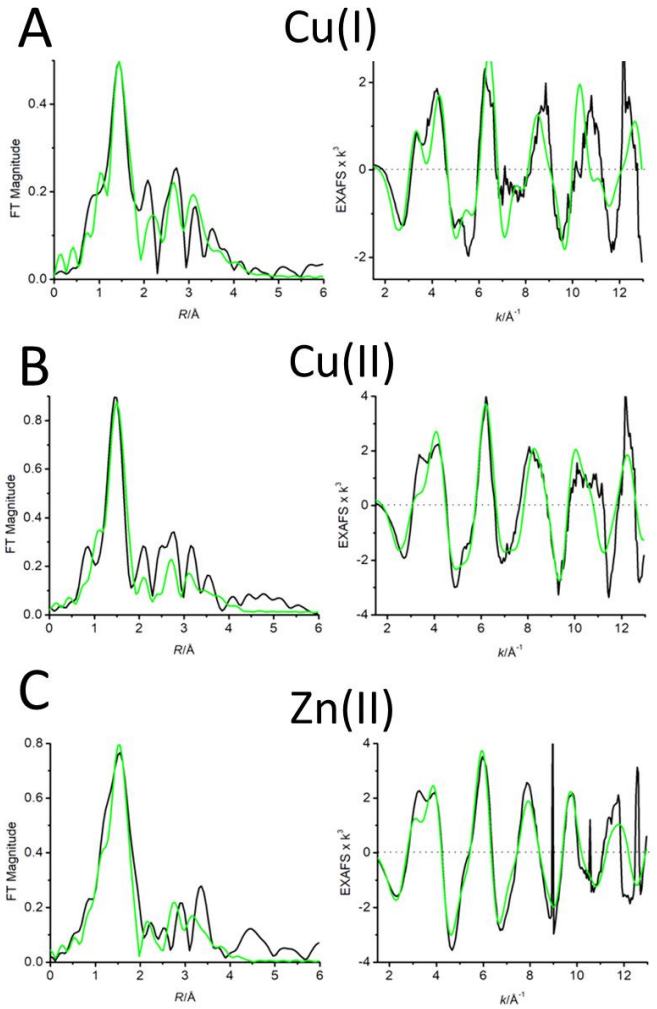

Figure S4. Fourier transforms of EXAFS (left) and EXAFS (right) for Cu(I) at pH 5.8 (A), Cu(II) at pH 5.8 (B), and Zn(II) at pH 9.5 (C) **GR**$W_{27stamAEL}$L33H. The data are shown in black and the fits are shown in green. The best fits shown are those discussed in the main text and highlighted in Table S1.

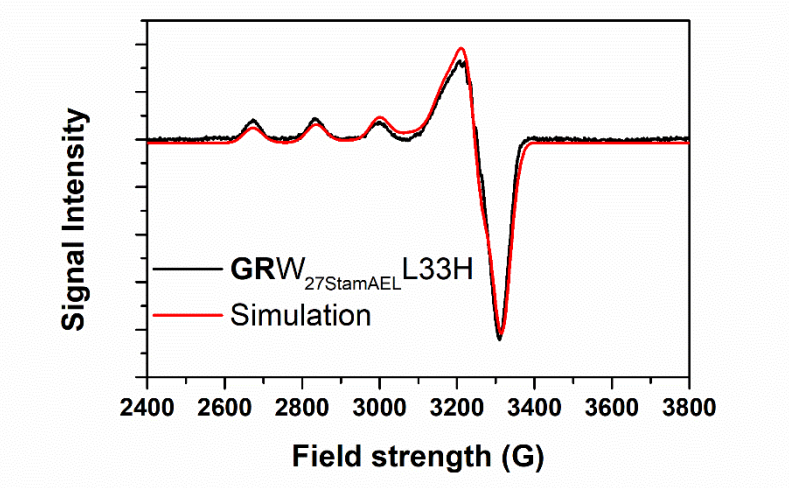

Figure S5. EPR spectra (black) and fit (red) of Cu(II) **GR**$W_{27stamAEL}$L33H at pH 5.8.

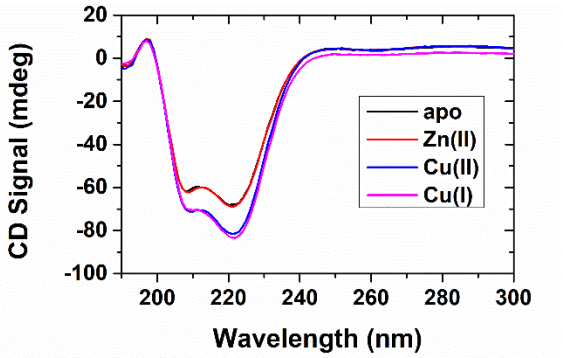

Figure S6. CD spectra collected for apo (black line), Zn(II)-bound (red line), Cu(II)-bound (blue line) and Cu(I) bound (magenta line) forms of **GR**$W_{27stamAEL}$L33H. Conditions: 3 accumulations, 9 μM peptide (3 μM 3SCC) in 10 mM potassium phosphate, pH 7.5. Metallated species had 3 μM of the respective metal added and then stirred for 10 mins at room temperature prior to data collection. The Cu(I) sample was prepared in degassed solutions in an anaerobic glove box in a sealed cuvette.

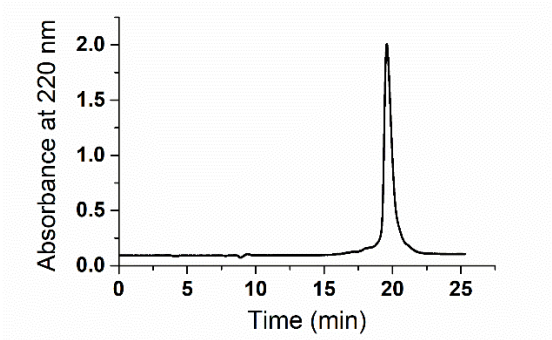

Figure S7. HPLC trace of purified **GR**$W_{27stamAEL}$L33H.

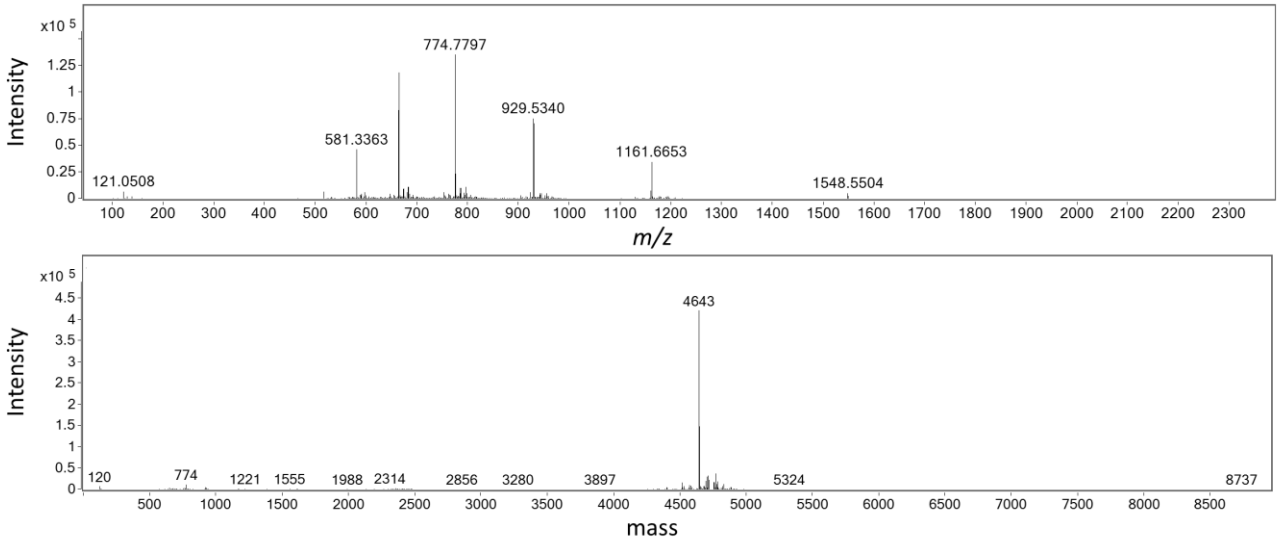

Figure S8. ESI mass spectral data collected for purified **GR**$W_{27stamAEL}$L33H. The upper panel shows the charge state distribution and the lower panel shows the deconvoluted mass. Calculated mass: 4643 Da, observed mass: 4643 Da.

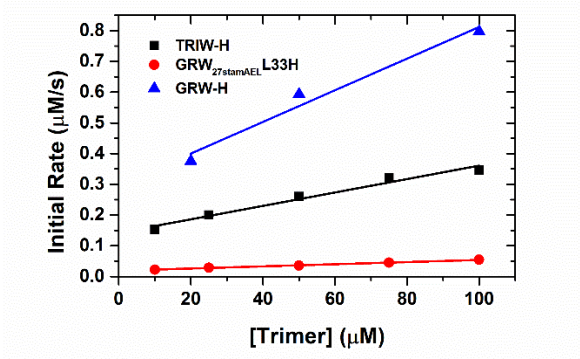

Figure S9. Pseudo first order kinetics of pNPA hydrolysis as a function of trimer concentration for TRI-H (black), **GR**W$_{27stamAEL}$L33H (red) and GRL30H (blue).

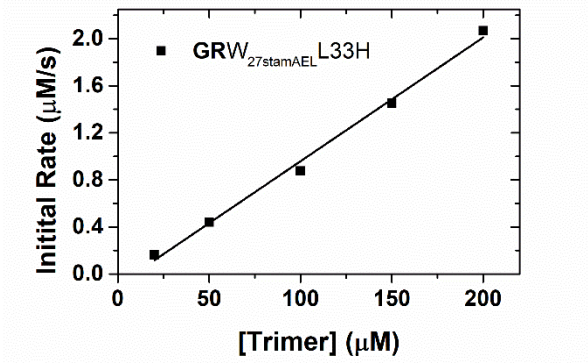

Figure S10. Pseudo-first order kinetics of CuNiR activity as a function of trimer concentration for **GR**W$_{27stamAEL}$L33H.

References

[1] L. Ruckthong, J. A. Stuckey, V. L. Pecoraro, *Methods Enzymol.* **2016**, *580*, 135-148.
[2] M. Hendrich, *SpinCount*; Carnegie Mellon University: Pittsburgh, PA, **2018.**
[3] Z. Xiao, F. Loughlin, G. N. George, G. J. Howlett, A. G. Wedd, *J. Am. Chem. Soc.* **2004**, *126*, 3081-3090.
[4] M. Tegoni, F. Yu, M. Bersellini, J. E. Penner-Hahn, V. L. Pecoraro, *Proc. Natl. Acad. Sci. U. S. A.* **2012**, *109*, 1-6.
[5] A. Kocyła, A. Pomorski, A. Krężel, *J. Inorg. Biochem.* **2017**, *176*, 53-65.
[6] M. L. Zastrow, V. L. Pecoraro, *J. Am. Chem. Soc.* **2013**, *135*, 5895-5903.
[7] F. Yu, J. E. Penner-Hahn, V. L. Pecoraro, *J. Am. Chem. Soc.* **2013**, *135*, 18096-18107.
[8] M. L. Zastrow, A. F. Peacock, J. A. Stuckey, V. L. Pecoraro, *Nat. Chem.* **2012**, *4*, 118.
[9] G. N. George, I. J. Pickering, *EXAFSPAK: A Suite of Computer Programs for Analysis of X-ray Absorption Spectra*; Available at http://ssrl.slac.stanford.edu/exafspak.html: **2000.**
[10] A. L. Ankudinov, J. Rehr, *Phys. Rev. B* **1997**, *56*, R1712.
[11] T.-C. Weng, G. S. Waldo, J. E. Penner-Hahn, *J. Synchrotron Radiat.* **2005**, *12*, 506-510.
[12] L. Ruckthong, M. L. Zastrow, J. A. Stuckey, V. L. Pecoraro, *J. Am. Chem. Soc.* **2016**, *138*, 11979-11988.
[13] E. Khazina, V. Truffault, R. Büttner, S. Schmidt, M. Coles, O. Weichenrieder, *Nat. Struct. Mol. Biol.* **2011**, *18*, 1006-1014.
[14] Schrodinger, LLC, **2015**.
[15] E. F. Pettersen, T. D. Goddard, C. C. Huang, G. S. Couch, D. M. Greenblatt, E. C. Meng, T. E. Ferrin, *J. Comput. Chem.* **2004**, *25*, 1605-1612.
[16] J. Wang, R. M. Wolf, J. W. Caldwell, P. A. Kollman, D. A. Case, *J. Comput. Chem.* **2004**, *25*, 1157-1174.
[17] J. Wang, W. Wang, P. A. Kollman, D. A. Case, *J. Mol. Graphics Modell.* **2006**, *25*, 247-260.
[18] K. J. Koebke, F. Yu, C. Van Stappen, T. B. Pinter, A. Deb, J. E. Penner-Hahn, V. L. Pecoraro, *J. Am. Chem. Soc.* **2019**.

Author Contributions

TBJP, and VLP designed the experiments. TBJP designed the stammer peptide sequence which was synthesized by ECM and TBJP. TBJP and ECM collected and analyzed the data for CD titrations, copper binding constants, and catalytic activities. AET collected and interpreted the data for zinc affinity and metallated CD spectra. XAS data were collected by TBJP, AET, KJK, and AD and analyzed by TBJP and KJK with assistance from AD, JEPH, and VLP. TBJP and KJK collected the EPR data which was analyzed and fit by ECM. TBJP and KJK created figures. TBJP and VLP wrote the manuscript with assistance and edits from all authors.